

# Synthesis and Characterization of Carboxyl-Functionalized Magnetic Nanogel via "Green" Photochemical Method

Jun Hong,<sup>1,2</sup> Peijun Gong,<sup>1,2</sup> Dongmei Xu,<sup>1,2</sup> Hanwen Sun,<sup>1,2</sup> Side Yao<sup>1</sup>

<sup>1</sup>Shanghai Institute of Applied Physics, Chinese Academy of Sciences, Shanghai 201800, People's Republic of China

<sup>2</sup>Graduate School of Chinese Academy of Sciences, Beijing 100039, People's Republic of China

Received 3 June 2006 ; accepted 14 October 2006

DOI 10.1002/app.25655

Published online 27 April 2007 in Wiley InterScience (www.interscience.wiley.com).

**ABSTRACT:** Carboxyl-functionalized magnetic nanogel was synthesized by facile "green" photochemical method. A possible mechanism of photochemical synthesis was proposed. Effects of irradiation time and volume of monomer dropped on the hydrodynamic diameter of the magnetic nanogel were investigated by photo correlation spectroscopy. The image of atomic force microscopy presented that the magnetic nanogel was with loosed structure. X-ray diffraction analysis showed that UV irradiation did not induce phase change of Fe<sub>3</sub>O<sub>4</sub>. Superparamag-

netic behaviors were retained for Fe<sub>3</sub>O<sub>4</sub> while slightly reducing the value of saturation magnetization for surface coating. High magnetic content of (as high as 85%) and strong magnetization of Fe<sub>3</sub>O<sub>4</sub> guaranteed that the magnetic nanogel was susceptible to external applied magnetic field. © 2007 Wiley Periodicals, Inc. *J Appl Polym Sci* 105: 1882–1887, 2007

**Key words:** magnetic polymers; photopolymerization; coating; gels

## INTRODUCTION

The integration of superparamagnetic materials and functional polymers has attracted an increasing interest because of its superparamagnetic property as well as other useful properties, offering potential applications in numerous areas such as RNA and DNA purification,<sup>1,2</sup> immobilized enzymes,<sup>3,4</sup> and magnetic resonance imaging (MRI) contrast agent.<sup>5,6</sup> The design and synthesis of functional superparamagnetic nanogels are the subjects of current research.

Hitherto, many types of organic materials such as natural macromolecules,<sup>7,8</sup> synthetic polymers<sup>9–12</sup> have been used as coating agents in the preparation of core-shell microspheres. Microspheres with polymeric coating layer have become increasingly attractive because they can be synthesized easily in a wide variety of compositions and can be also modified for further applications. Nowadays, several methods, including microemulsion polymerization,<sup>13</sup> emulsion polymerization,<sup>14</sup> and *in situ* polymerization<sup>15</sup> have been developed to prepare magnetical microspheres with core-shell structure.

Based on the investigation of the photo-polymerization process of vinyl monomers in alcohol, Hoffmann et al.<sup>16</sup> and Stroyuk et al.<sup>17</sup> found out that quantum-sized semiconductor particles were efficient photoini-

tiators to initiate polymerization of monomers in high quantum yields and proposed the mechanisms of polymerization. Therefore, it was possible to synthesize core-shell magnetic nanogels via photochemical method using quantum-sized Fe<sub>3</sub>O<sub>4</sub> nanoparticles as photoinitiator. Actually, magnetic nanogels with amino groups<sup>18</sup> or hydroxyl groups<sup>19</sup> had been synthesized via photochemical method in our group and successfully applied in the targeted radiopharmaceutical application and biosensor.

Compared with other methods reported, photochemical method was endowed with a number of advantages. For example, properties including particle size and polymeric extent of the synthesized magnetic nanogels could be conveniently controlled by changing the volume of monomer dropped, irradiation time, and suchlike. Most importantly, the reaction medium was free of initiator and stabilizer, namely, friendly to environment. In this sense, photochemical method represented a facile and "green" process in preparation of magnetic nanogels in a wide variety of compositions.

In the present study, carboxyl-functionalized magnetic nanogel was prepared by photochemical method, and characterized by use of FTIR spectroscopy, atomic force microscopy (AFM), photo correlation spectroscopy (PCS), X-ray diffraction (XRD) analysis, and vibrating sampling magnetometer (VSM) measurement.

Correspondence to: S. Yao (yaoside@sinap.ac.cn).

Contract grant sponsor: Science and Technology Commission of Shanghai Municipality; contract grant number: No.0352nm120.

## EXPERIMENTAL

### Materials

Methylacrylic acid (MAA) and absolute alcohol were of analytic grade and purchased from Shanghai

*Journal of Applied Polymer Science*, Vol. 105, 1882–1887 (2007)  
©2007 Wiley Periodicals, Inc.

Chemical Reagents. MAA was purified prior to use. Water was doubly distilled after deionization. 500 W xenon lamp was purchased as irradiation source.

### Preparation of Fe<sub>3</sub>O<sub>4</sub> nanoparticles

Superparamagnetic Fe<sub>3</sub>O<sub>4</sub> nanoparticles were synthesized via partial reduction method according to references.<sup>20,21</sup> The procedures were as follows: FeCl<sub>3</sub>·6H<sub>2</sub>O (3.3 g) was dissolved in 100 mL of water. The solution was adjusted to pH 2 before charging it into a 500 mL of three-necked flask. With an injector, 50 mL of 0.16M sodium sulfite solution, which was freshly prepared, was added slowly into the flask. After the red solution changed its color to yellow, 40 mL of diluted ammonia (12 mL of concentrated ammonia was diluted with 28 mL water) was rapidly injected into the flask, while stirring and bubbling intensively with nitrogen gas as protective gas. The reaction was kept at 60°C for 30 min, before being matured for about 2 h at room temperature. After completion of the reaction, the black magnetic precipitate was magnetically concentrated and washed several times with water. Finally, Fe<sub>3</sub>O<sub>4</sub> nanoparticles were redispersed in aqueous solution. The obtained Fe<sub>3</sub>O<sub>4</sub> nanoparticles were about 10 nm in diameter, with a polydispersity index of 0.187. Saturation magnetization was determined to be 66.3 emu g<sup>-1</sup>, coercivity and remanence were close to zero.

### Synthesis of carboxyl-functionalized magnetic nanogel

The carboxyl-functionalized magnetic nanogel was synthesized via photochemical method. Certain volume of MAA and 2 mL of alcohol (served as chain transfer agent) were mixed well in 120 mL of water, and adjusted the solution pH to 7.5 with 5M NaOH before charging into the quartz flask, then bubbling nitrogen gas for 10 min to deaerate. 2.5 mL of ferrofluid (8.0 mg mL<sup>-1</sup>) was dropped into the flask. The reaction was kept for minutes under xenon lamp irradiation. After completion of the photochemical synthesis, the magnetic nanogel was isolated by a magnet and washed several times with water.

### Measurements

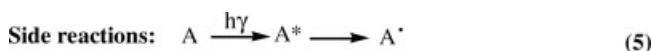
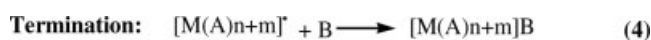
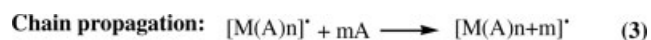
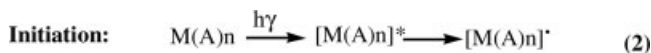
Size distribution and zeta potential of the magnetic nanogel were determined by a Zetasizer 3000HS PCS (Malvern Instruments). Morphology of the magnetic nanogel was investigated with an AFM (Nanoscope IIIa, Digital Instruments) using tapping mode with a standard silicon nitride tip. The proof coating of MAA onto Fe<sub>3</sub>O<sub>4</sub> nanoparticles was confirmed by an Avatar 370 FTIR spectrophotometer (Nicolet, USA). Thermogravimetric analysis was determined by a simultaneous DTA-TG (Shimadzu, DTG-60M) and DSC apparatus

(Shimadzu, DSC-60) by heating the samples from room temperature to 700°C under N<sub>2</sub> atmosphere at a heating rate of 10°C min<sup>-1</sup>. Magnetic properties of the samples were obtained with a Princeton Applied Research VSM model 155 and a Quantum Design SQUID MPMS-XL (ac and dc modes and maximum static field 5 T). Powder XRDs were recorded on a D/max 2550V X-ray diffractometer (Cu K $\alpha$  radiation,  $\lambda = 1.5418\text{\AA}$ ).

## RESULTS AND DISCUSSION

### Synthesis of carboxyl-functionalized magnetic nanogel

The carboxyl-functionalized magnetic nanogel was synthesized via photochemical method. Fe<sub>3</sub>O<sub>4</sub> and MAA were mixed in a quartz flask. Part of MAA was adsorbed by Fe<sub>3</sub>O<sub>4</sub> nanoparticles because of the larger surface-to-volume ratio before being irradiated. In the experiment, xenon lamp, whose irradiation spectrum was consecutive, was used as irradiation source. As the molar extinction coefficient of Fe<sub>3</sub>O<sub>4</sub> was much larger than that of MAA in ultraviolet region, therefore, a majority of photons were adsorbed by Fe<sub>3</sub>O<sub>4</sub> nanoparticles when the reaction system was exposed to UV light emitted by xenon lamp. Holes<sup>22</sup> were subsequently generated on the surface of Fe<sub>3</sub>O<sub>4</sub> nanoparticles. They had intensive liability to capture MAA adsorbed on the surface of Fe<sub>3</sub>O<sub>4</sub> nanoparticles. Free radical, which was composed of Fe<sub>3</sub>O<sub>4</sub> nanoparticles and monomer adsorbed on the Fe<sub>3</sub>O<sub>4</sub> nanoparticle, was generated. Free radical then combined with free MAA in the solution, and initiated the chain propagation. The chain propagation was terminated by the active species of free radical existing in the system. Minority of MAA (free radical) could be directly generated by UV light irradiation. Side reactions, including homopolymerization of MAA and aggregation of magnetic nanogels, were involved in the reaction system. The possible mechanism of photochemical synthesis could be illuminated with the following equations:



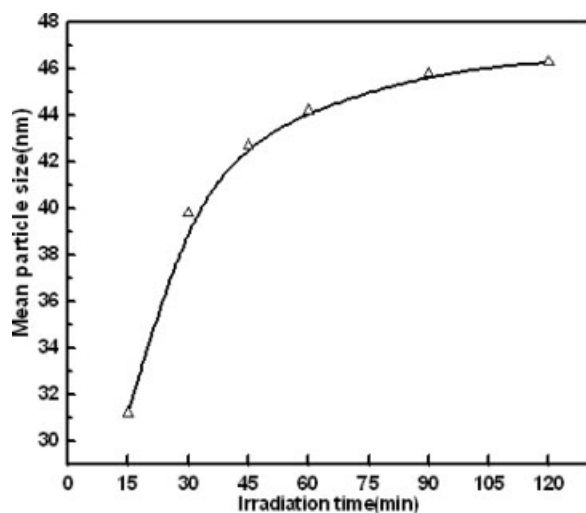
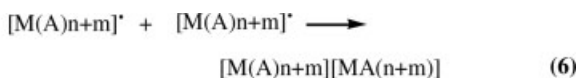


**Figure 1** Effect of irradiation time on the mean particle size of the magnetic nanogel.



A	free monomer of MAA in the solution
M	Fe <sub>3</sub> O <sub>4</sub> nanoparticle
B	free radical
M(A)n	MAA adsorbed on the Fe <sub>3</sub> O <sub>4</sub> nanoparticle
[M(A)n]*	excitation state of monomer adsorbed on the Fe <sub>3</sub> O <sub>4</sub> nanoparticle
A*	excitation state of monomer
A•	free radical of MAA
[M(A)n]•	free radical of MAA adsorbed on the Fe <sub>3</sub> O <sub>4</sub> nanoparticle
[M(A)n+m]B	magnetic nanogel
[M(A)n+m][M(A)n+m]	aggregated magnetic nanogel
(A)y+1	homo+polymer of MAA

Effect of variation of irradiation time on the mean hydrodynamic particle size of the magnetic nanogel was evaluated by PCS determination. As shown in Figure 1, the mean particle size increased from 31 to 46 nm within 2 h while 1 mL of MAA was dropped into the flask. This indicated that the thickness of polymer layer had been increasing continuously because of the propagation of MAA on the surface of Fe<sub>3</sub>O<sub>4</sub> nanoparticles. Nevertheless, a slow increasing trend was observed when the irradiation time was over 45

min. With the reaction proceeding, the monomer in the reaction system kept decreasing, and led to decrease of the rate of chain propagation. At the same time, viscosity of the reaction system was enhanced by the synthesized magnetic nanogel and by-products, and resulted in the probability of chain propagation decreased. The two reasons earlier made the increment of particle size of the magnetic nanogel decrease.

Considering the balance between particle size and polymeric extent of the magnetic nanogel, 30 min was selected as suitable irradiation time.

Based on the chosen irradiation time, dependence of hydrodynamic diameter of the magnetic nanogel on the volume of monomer dropped [ $V_{MAA}$ (dropped)] was investigated. Mean hydrodynamic diameter of the magnetic nanogel ranged from 10 to 33 nm when  $V_{MAA}$ (dropped) varied from 0 to 1.25 mL (Fig. 2). During the synthesis, hydrodynamic diameter of the magnetic nanogel kept increasing when there was some residual monomer in the reaction system. Accordingly, mean particle size was greatly dependent on the volume of monomer dropped.

#### Chemical composition of the carboxyl-functionalized magnetic nanogel

Figure 3 was FTIR spectrum of the magnetic nanogel. The presence of Fe<sub>3</sub>O<sub>4</sub> could be identified by the strong absorption band around 579 cm<sup>-1</sup>, which corresponded to the Fe—O bond of naked Fe<sub>3</sub>O<sub>4</sub>. The bands of 1749 and 1162 cm<sup>-1</sup> were assigned to the C=O and C—O stretching vibrations of carbonyl group. The wide band of 3600–3300 cm<sup>-1</sup> corresponded to the O—H stretching vibration of MAA and water

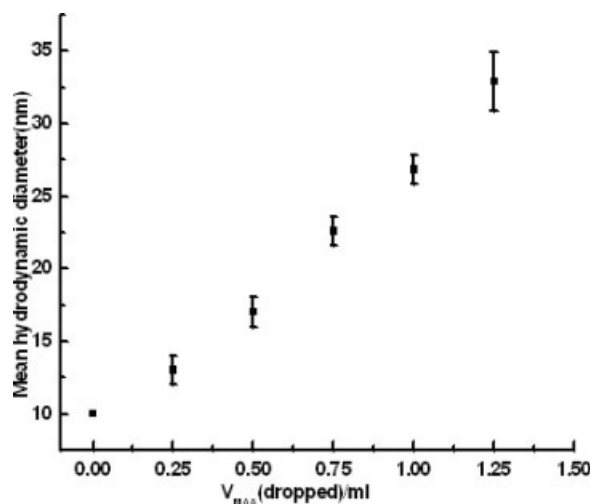


**Figure 2** Dependence of mean particle size of the magnetic nanogel on volume of monomer dropped.

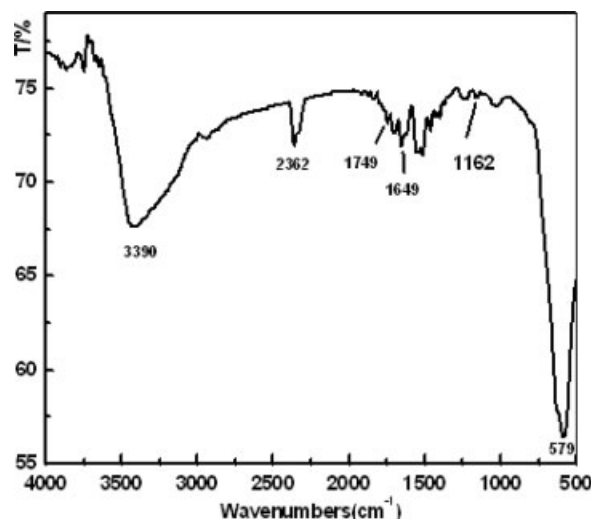


**Figure 3** FTIR spectrum of the carboxyl-functionalized magnetic nanogel.

(including bound water). On the other hand, the magnetic nanogel was magnetically concentrated and washed with water several times after synthesis to eliminate the interference of homopolymer. The results above revealed that MAA was coated on the surface of Fe<sub>3</sub>O<sub>4</sub> nanoparticles successfully.

Crystalline structure of the carboxyl-functionalized magnetic nanogel was illustrated in Figure 4. The six characteristic peaks occurred at 2θ of 30.1, 35.5, 43.2, 53.5, 57.0, and 62.8, represent corresponding indices (220),(311),(400),(422),(511), and (440), respectively, of Fe<sub>3</sub>O<sub>4</sub> according to standard XRD data cards of Fe<sub>3</sub>O<sub>4</sub> crystal (JCPDS No. 19-0629). This revealed that crystalline structure of Fe<sub>3</sub>O<sub>4</sub> was not affected by UV irradiation, namely, core of the carboxyl-functionalized magnetic nanogel was Fe<sub>3</sub>O<sub>4</sub>.

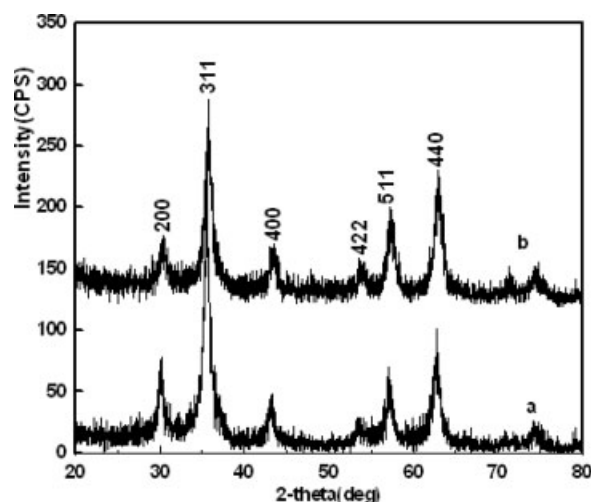


**Figure 4** XRD patterns of (a) Fe<sub>3</sub>O<sub>4</sub>, (b) carboxyl-functionalized magnetic nanogel.

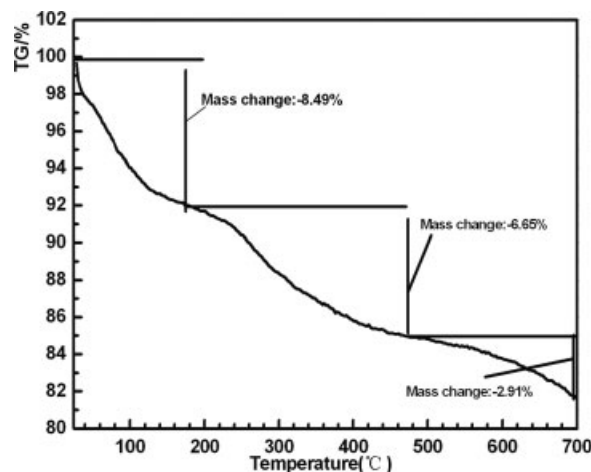


**Figure 5** TG curve of the carboxyl-functionalized magnetic nanogel.

As presented in Figure 5, an 8.5% weight loss of the magnetic nanogel was observed in the temperature range from room temperature to 120°C. This indicated that water (including bound water) was contained in the magnetic nanogel. The polymeric shell was decomposed at about 180°C and finished at about 460°C. The polymeric extent was determined to be 6.7%. Magnetic content of Fe<sub>3</sub>O<sub>4</sub> was calculated to be 84.9% in dried state.

**Particle size and morphology**

The carboxyl-functionalized magnetic nanogel was about 16 nm in diameter, with a polydispersity index of 0.347 [Fig. 6, 5<sub>MAA</sub>(dropped) = 0.5 mL, irradiation time = 30 min], which was broader than that of the Fe<sub>3</sub>O<sub>4</sub> core (0.187). This might be caused by by-prod-

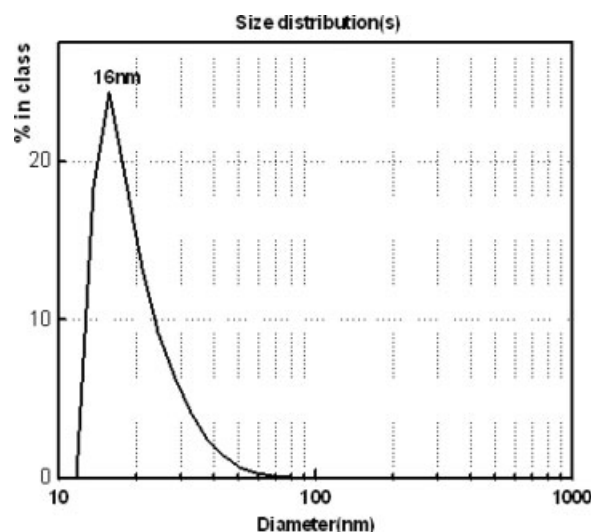


**Figure 6** Size distribution of the magnetic nanogel measured by PCS.

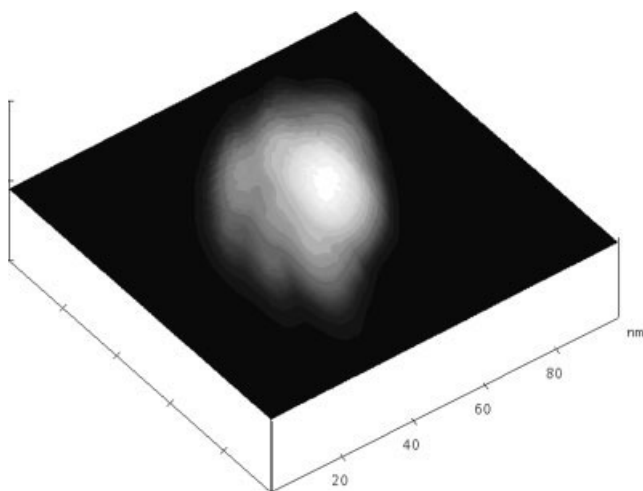


**Figure 7** AFM image of the carboxyl-functionalized magnetic nanogel.

uct of photochemical synthesis (aggregated magnetic nanogel) and could be improved by centrifugation.

Using XRD data, the average crystal size in diameter of the carboxyl-functionalized magnetic nanogel could be estimated using Debye–Scherrer formula:

$$D(hkl) = \frac{0.9 \times \lambda}{\beta \times \cos \theta}$$

where  $\lambda$  represents the X-ray wavelength ( $1.5418\text{\AA}$ ),  $\beta$  is FWHM (full-width at half-maximum) of peaks,  $\theta$  is the Bragg angle,  $D(hkl)$  is the calculated crystal size in diameter.

From its reflection of (311) (see Fig. 4),  $D(hkl)$  was calculated to be 12.8 nm. The difference in particle size between PCS determination and XRD analysis was arising from the two different measurements. PCS was usually used in determination of hydrodynamic diameter of nanoparticles while Debye–Scherrer formula was used to estimate average crystal size in dried state. Accordingly, particle size obtained by PCS was undoubtedly larger than  $D(hkl)$  because of the hydrated layer.

It is known that the condition for superparamagnetism is  $KV \gg kT$ , where  $KV$  is the anisotropy energy and  $kT$  is the thermal agitation energy. When size of the magnetic crystallite is below the critical size of 25 nm,<sup>17</sup> the magnetic crystallite exhibits superparamagnetic behaviors. According to the values of particle size obtained by PCS determination and XRD analysis, the magnetic nanogel should be superparamagnetic. Nevertheless, it was needed to be proved by further VSM measurement.

Since the reaction medium was free of crosslinker, thus tight polymeric crosslinked network could not be formed on the surface of  $\text{Fe}_3\text{O}_4$  nanoparticles and surface of the synthesized magnetic nanogel should be with loosed structure. This assumption was confirmed

by the evidence of AFM image (Fig. 7), and core-shell structure was clearly obtained.

### Magnetic properties

Magnetic properties of carboxyl-functionalized magnetic nanogel were measured by VSM. Saturation magnetization of the magnetic nanogel was measured to be  $61.6 \text{ emu g}^{-1}$ . The immeasurable coercive and remanence suggested that superparamagnetic properties were retained for  $\text{Fe}_3\text{O}_4$  after surface coating (Fig. 8). These data confirmed the conclusion that the magnetic nanogel was superparamagnetic drawn by use of particle size of the magnetic nanogel.

Taking into account the polymeric coating layer and a trace amount of water (including bound water), saturation magnetization of the carboxyl-functionalized magnetic nanogel was calculated to be  $65.1 \text{ emu g}^{-1}$ , which was slightly decreased in comparison with that of naked  $\text{Fe}_3\text{O}_4$  because of surface coating.<sup>23</sup> Another tendency towards lower magnetization might be the oxidation of the surface of magnetite during the polymerization process, which led to the formation of a trace amount of maghemite, whose saturation magnetization ( $76 \text{ emu g}^{-1}$ ) was lower than that of bulk magnetite ( $92 \text{ emu g}^{-1}$ ).

Furthermore, excellent magnetic response, which was desirable for magnetic separation, was guaranteed by the high magnetic content and strong magnetization of  $\text{Fe}_3\text{O}_4$ .

### Zeta potential

With respect to zeta potential, it plays an important role in the stability of nanoparticles. It is reported that isoelectrical point of  $\text{Fe}_3\text{O}_4$  is about pH 7.0, and hence  $\text{Fe}_3\text{O}_4$  nanoparticles inclined to aggregation under

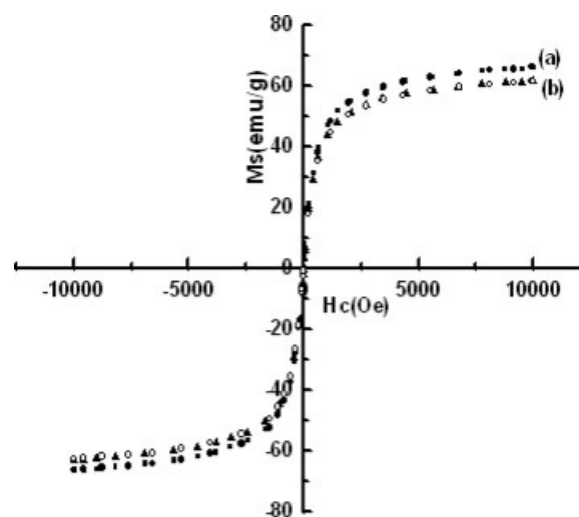


**Figure 8** Hysteresis loops of (a)  $\text{Fe}_3\text{O}_4$ , (b) carboxyl-functionalized magnetic nanogel.

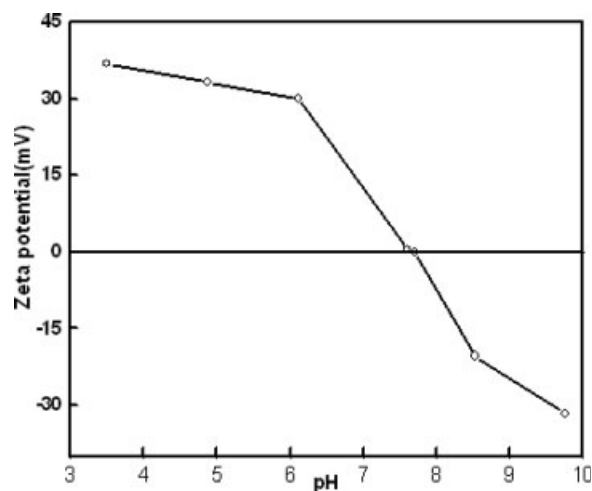


Figure 9 Zeta potential curve measurements versus pH.

neutral condition. As shown in Figure 9, isoelectrical point of the carboxyl-functionalized magnetic nanogel was determined to be pH 7.7. The magnetic nanogel had a zeta potential of +19 mV in comparison with 0 mV of  $\text{Fe}_3\text{O}_4$  at pH 7. It was anticipated that the carboxyl-functionalized magnetic nanogel had better stability than naked  $\text{Fe}_3\text{O}_4$  nanoparticles under neutral surrounding condition, and polymeric coating layer could provide stability against aggregation for the magnetic nanogel.

### CONCLUSIONS

In this article, carboxyl-functionalized magnetic nanogel was synthesized via photochemical method. The carboxyl-functionalized magnetic nanogel was with loosed structure. Average hydrodynamic diameter of the magnetic nanogel could be manipulated by varying the irradiation time, volume of monomer dropped and so on. Crystalline structure of  $\text{Fe}_3\text{O}_4$  was not affected by xenon lamp irradiation and surface coating. The magnetic nanogel behaved superparamagnetic. Photochemical method represented an economical and facile "green" process for preparation of functional magnetic nanogels in a wide variety of

compositions. The synthesized magnetic nanogels with functional groups could be utilized as carriers in enzyme immobilization, biosensor, and MRI contrast agent and suchlike in future.

### References

1. Koneracká, M.; Kopřivná, P.; Antálík, M.; Timko, M.; Ramchand, C.N.; Lobo, D. Mehta, RV.; Upadhyay, RV. *J Magn Magn Mater* 1999, 201, 427.
2. Elaïssari, A. Bourrel, V. *J Magn Magn Mater* 2001, 225, 151.
3. Dyal, A. Loos, K. Noto, M. Chang, S.W.; Spagnoli, C. Shafi, K.V.P.M.; Ulman, A. Cowman, M. Gross, RA. *J Am Chem Soc* 2003, 125, 1684.
4. Konno, T.; Watanabe, J.; Ishihara, K. *Biomacromolecules* 2004, 5, 342.
5. Häfeli, U.O.; Sweeney, S.M.; Beresford, B.A.; Sim, E.H.; Macklis, R.M. *J Biomed Mater Res* 1994, 28, 901.
6. Ito, A.; Shinkai, M.; Honda, H.; Kobayashi, T. *J Biosci Bioeng* 2005, 100, 1.
7. Fei, B.; Lu, H.F.; Xin, J.H. *Polymer* 2006, 47, 947.
8. Basinska, T. *Macromol Biosci* 2005, 5, 1145.
9. Feng, X.M.; Mao, C.J.; Yang, G. Hou, W.H.; Zhu, J.J. *Langmuir* 2006, 22, 4384.
10. Karim, M.R.; Lee, C.J.; Lee, MS. *J Polym Sci Part A: Polym Chem* 2006, 44, 5283.
11. İlhan, U.F.; Fabrizio, E.F.; McCorkle, L.; Scheiman, D.A.; Dass, A.; Palczar, A.; Meador, MB.; Johnston, J.C.; Leventis, N. *J Mater Chem* 2006, 16, 3046.
12. Kumar, V.R.R.; Pradeep, T. *J Mater Chem* 2006, 16, 837.
13. Csetneki, I.; Kabai Faix, M.; Szilágyi, A.; Kovács, AL.; Németh, Z.; Zrinyi, M. *J Polym Sci Part A: Polym Chem* 2004, 42, 4802.
14. Noguchi, H.; Yanase, N.; Uchida, Y. *Appl Polym Sci* 1993, 48, 1539.
15. Sharma, R.; Lamba, S.; Annapoorni, S. *J Phys D: Appl Phys* 2005, 38, 3354.
16. Hoffman, A.J.; Mills, G.; Yee, H. *J Phys Chem* 1992, 96, 5546.
17. Stroyuk, A.L.; Granchak, V.M.; Korzhak, A.V.; Kuchmii, SY. *J Photochem Photobiol A* 2004, 162, 339.
18. Sun, H.W.; Yu, J.H.; Gong, P.J.; Xu, D.M.; Zhang, C.F.; Yao, S.D. *J Magn Magn Mater* 2005, 294, 273.
19. Gong, P.J.; Yu, J.H.; Sun, H.W.; Hong, J.; Zhao, S.F.; Xu, D.M.; Yao, S.D. *J Appl Polym Sci* 2006, 101, 1283.
20. Cao, J.Q.; Wang, Y.X.; Yu, J.F.; Xia, J.Y.; Zhang, C.F.; Yin, D.Z.; Häfeli, U.O. *J Magn Magn Mater* 2004, 277, 165.
21. Qu, S.C.; Yang, H.B.; Ren, D.W.; Kan, S.H.; Zou, G.T.; Li, D.M.; Li, M.H. *J Colloid Interface Sci* 1999, 215, 190.
22. Behar, D.; Rabani, J. *J Phys Chem B* 2001, 105, 6324.
23. Yamaura, M.; Camilo, R.L.; Sampaio, L.C.; Macêdo, M.A.; Nakamura, M.; Toma, H.E. *J Magn Magn Mater* 2004, 279, 210.